Evaluation of Optimal Net Load Management in Microgrids Using Hardware-in-the-Loop Simulation

Preprint

Jing Wang,[1] Soham Chakraborty,[1,2] Vivek Khatana,[2]
Blake Lundstrom,[3] Govind Saraswat,[1] and Murti Salapaka[2]

1 National Renewable Energy Laboratory
2 University of Minnesota
3 Enphase Energy

Presented at the IEEE PES Innovative Smart Grid Technologies Conference (ISGT NA)
New Orleans, Louisiana
April 24–28, 2022

NREL is a national laboratory of the U.S. Department of Energy
Office of Energy Efficiency & Renewable Energy
Operated by the Alliance for Sustainable Energy, LLC

This report is available at no cost from the National Renewable Energy Laboratory (NREL) at www.nrel.gov/publications.

Contract No. DE-AC36-08GO28308

Conference Paper
NREL/CP-5D00-80839
May 2022

Evaluation of Optimal Net Load Management in Microgrids Using Hardware-in-the-Loop Simulation

Preprint

Jing Wang,[1] Soham Chakraborty,[1,2] Vivek Khatana,[2]
Blake Lundstrom,[3] Govind Saraswat,[1] and Murti Salapaka[2]

1 National Renewable Energy Laboratory
2 University of Minnesota
3 Enphase Energy

Suggested Citation
Wang, Jing, Soham Chakraborty, Vivek Khatana, Blake Lundstrom, Govind Saraswat, and Murti Salapaka. 2022. *Evaluation of Optimal Net Load Management in Microgrids Using Hardware-in-the-Loop Simulation: Preprint*. Golden, CO: National Renewable Energy Laboratory. NREL/CP-5D00-80839. https://www.nrel.gov/docs/fy22osti/80839.pdf.

NREL is a national laboratory of the U.S. Department of Energy
Office of Energy Efficiency & Renewable Energy
Operated by the Alliance for Sustainable Energy, LLC

This report is available at no cost from the National Renewable Energy Laboratory (NREL) at www.nrel.gov/publications.

Contract No. DE-AC36-08GO28308

Conference Paper
NREL/CP-5D00-80839
May 2022

National Renewable Energy Laboratory
15013 Denver West Parkway
Golden, CO 80401
303-275-3000 • www.nrel.gov

NOTICE

This work was authored in part by the National Renewable Energy Laboratory, operated by Alliance for Sustainable Energy, LLC, for the U.S. Department of Energy (DOE) under Contract No. DE-AC36-08GO28308. This material is based upon work supported by the U.S Department of Energy, Advanced Research Projects Agency–Energy under grant DE-AR0001016. The views expressed herein do not necessarily represent the views of the DOE or the U.S. Government.

Cover Photos by Dennis Schroeder: (clockwise, left to right) NREL 51934, NREL 45897, NREL 42160, NREL 45891, NREL 48097, NREL 46526.

Evaluation of Optimal Net Load Management in Microgrids Using Hardware-in-the-Loop Simulation

Jing Wang[1], Soham Chakraborty[1,2], Vivek Khatana[2], Blake Lundstrom[3], Govind Saraswat[1], Murti Salapaka[2]
[1]Power Systems Engineering Center, National Renewable Energy Laboratory Golden, CO 80401, USA
[2]Electrical and Computer Engineering, University of Minnesota, Minneapolis, MN 55455, USA
[3]Enphase Energy, Austin, TX 78758, USA
Jing.Wang@nrel.gov, murtis@umn.edu

***Abstract*—This paper presents the performance evaluation of a net load management (NLM) engine that balances load and generation in an isolated community to power a critical facility after a grid interruption event (e.g., the loss of a large generation unit). This NLM engine is particularly important for microgrid systems because it provides a high-speed, cost-optimal control solution to coordinate grid-forming inverters and to dispatch grid-following inverters and deferrable loads in microgrid systems to enhance grid resilience and reliability. The NLM algorithm cost-optimally dispatches the grid-following inverters and deferrable loads based on the demanded power and load priorities, and the grid-forming inverters use droop control to form system voltages and share active and reactive power. A controller-hardware-in-the-loop platform is developed to evaluate the control performance of the NLM algorithm with two sequential contingency events of lost generation units. The experimental results indicate that the NLM engine can maintain system stability, achieve the targeted system voltage and frequency, and balance load and generation to serve the critical facility with improved system resilience and reliability.**

Index Terms*— *Droop control, grid-forming inverter, grid-following inverter, net load management.

I. Introduction

The integration of distributed energy resources (DERs), such as solar photovoltaics (PV), into electric grids has increased significantly during recent years to meet renewable energy targets [1]. With the proliferation of DERs in electric grids, many utilities face challenges integrating large numbers of nonutility devices into operations at all levels and ensuring grid stability and controls over them; therefore, utilities are deploying emerging technologies, such as distributed energy management systems (DERMS), to improve the controllability and visibility of DERs [2]. Further, the intermittent and unpredictable nature of renewable generation makes supply uncertain, which, in turn, requires continuous net load balancing to ensure grid stability and viable operations.

A novel ramp rate control and active power smoothing technique is developed in [3] by shifting between PV and energy storge for net load profiles in large distribution networks where high levels of PV penetration exist. Based on historical data of load and DER generation, reference [4] investigates the potential future change in the net load variability considering increasing shares of wind and solar generation to find a solution for net load balancing. Similarly, a probabilistic day-ahead net load forecasting method using Bayesian deep learning is developed in [5] to capture both epistemic uncertainty and aleatoric uncertainty caused by the increasing integration of renewable generation.

Managing microgrid net load variability also attracts extensive research attention. Reference [6] investigates and compares two options to reduce microgrid net load variability resulting from high penetrations of renewable generation via local and central management. Reference [7] develops an algorithm to determine a bounded (near-optimal) curtailment strategy while simultaneously satisfying practical constraints on strategy switching overhead and curtailment fairness/priority. Residential demand management using deferrable loads and DER dispatch is developed in [8] to smooth net load demand variation caused by the large-scale integration of renewable energy resources.

Even though the mentioned literature has developed solutions/techniques for net load management (NLM) and prediction in distribution systems and microgrids, the work is more site specific. A versatile NLM algorithm is developed in [9] that can be used to provide a fast frequency response via optimal coordination of net load resources, and it can be extended for many other applications. This paper extends the NLM algorithm to dispatching DERs and deferrable loads in isolated communities, and the focus is to demonstrate the viability and stability of the NLM strategy via laboratory controller-hardware-in-the-loop (CHIL) evaluation. The contributions of this paper can be summarized as follows: 1) We model the real-world power system with grid-forming (GFM) and droop-controlled grid-following (GFL) inverters in electromagnetic transient (EMT) simulations, and we show the strategy of stabilizing the isolated system; 2) we present the details of expanding the NLM algorithm for load and generation management in the isolated system; and 3) we evaluate the NLM algorithm using CHIL and a real-world network model running in real time, which provides realistic laboratory testing results and proves the concept of NLM for the viable and stable operation of isolated systems.

II. Overview of the Hardware-in-the-Loop Setup

The overall setup of the hardware-in-the-loop (HIL) platform is presented in Fig. 1, which includes three main elements: the real-time simulation in the digital real-time simulator OPAL-RT, the NLM engine in a computer, and the current control algorithm for GFL inverters in TI DSPs. Note that the measurements and control commands are exchanged between OPAL-RT and the NLM engine through User

This work was authored in part by the National Renewable Energy Laboratory, managed and operated by Alliance for Sustainable Energy, LLC, for the U.S. Department of Energy (DOE) under Contract No. DE-AC36-08GO28308. This material is based upon work supported by the U.S Department of Energy, Advanced Research Projects Agency–Energy under grant DE-AR0001016. The views expressed in the article do not necessarily represent the views of the DOE or the U.S. Government. The U.S. Government retains and the publisher, by accepting the article for publication, acknowledges that the U.S. Government retains a nonexclusive, paid-up, irrevocable, worldwide license to publish or reproduce the published form of this work, or allow others to do so, for U.S. Government purposes.

Datagram Protocol (UDP). Each element is described in a separate section.

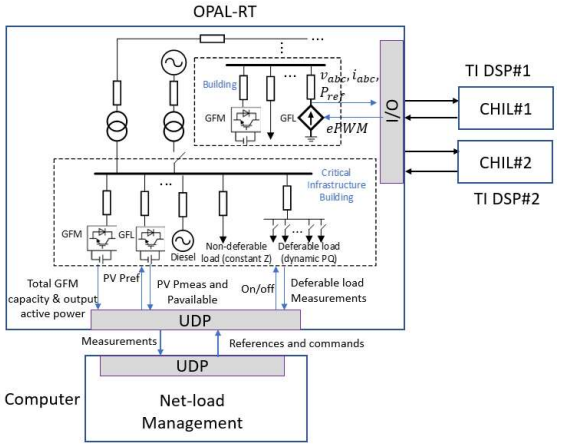

Fig. 1. Overview diagram of the integrated HIL platform.

III. Description of the Microgrid Model

The simulated electrical network is developed based on a real power network at the University of Minnesota campus, which has many buildings (here, we simulate eight buildings for the NLM evaluation, and we amend them with extra renewable resources for demonstration purposes), and each building connects multiple DERs and both deferrable as well as nondeferrable loads. The schematic diagram of the electrical network is shown in Fig. 2. This power network can connect with the utility grid under normal operation, and it can also work in fully autonomous mode because the network has multiple GFM sources in case the utility power is not available. The utility voltage source and its buses have a voltage level of 13.8 kV, and the buildings have a voltage level of 480 V. The service transformers are connected between the utility voltage and the buildings. All the elements in the system are three-phase. The building csCIu (commercial scale critical infrastructure unit) is the medical centre at the University of Minnesota, csCIu, is a critical facility and needs uninterruptible power supply. Nearby buildings that form the central core for this neighbourhood are called central core units (CCus). There are six CCu buildings, as shown in Fig. 2. MOB1 is a mobile auxiliary generation unit available near the University of Minnesota campus.

To better understand the simulated system, the power capacity ratings of the DERs and loads are listed in Table 1. Based on the calculation, we can understand the following: 1) the total generation power (400 kVA) is less than the total demand (750 kVA) of the critical facility, csCIu 2) Cold load is connected to Bus 5, and the cold load needs to be connected to the system all the time. For each building, the nondeferrable load is always connected to the system and cannot be interrupted. 3) The capacity of the nondeferrable load in each building is smaller than the available power generation capacity. 4) The total must-serve load capacity is 1140 kVA, and the total generation capacity is 1505 kVA.

The whole system is simulated in eMegaSim in OPAL-RT with a simulation time step of 100 µs. Each DER unit has a detailed control algorithm implemented, such as a phase-locked loop, Park transformation, droop control, power calculation, voltage control, and current control. The average inverter model is used to avoid any additional computational burden. The detailed model of the DERs adds huge computational complexity to the simulation model. To allow for the real-time simulation, the model is partitioned into five groups using the Artemis-SSN Nodal Interface Block in the OPAL-RT Artemis library. The V-type (left and right) interface is selected because the partitioned subsystems are connected to the rest of the system through a line impedance that is inductive. For each subsystem, the maximum allowable number of switches is 10 (single phase). So, the switches that do not change status during the simulation are deleted to keep the number of switches inside each subsystem within 10.

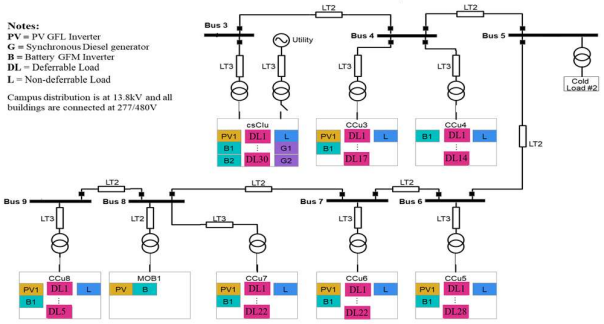

Fig. 2. Schematic diagram of the simulated microgrid in OPAL-RT.

Table 1: Net Load Resource Power Capacity Ratings

Net Load Type	Net Load Resource Power Capacity (kVA) **								
	csCIu	CCu 3	CCu 4	CCu 5	CCu 6	CCu 7	CCu 8	MOB1	Cold Load 2
PV1	100	50	-	100	100	50	100	50	-
B1	100	25	100	80	200	100	50	100	-
B2	100	-	-	-	-	-	-	-	-
G1/G2	50	-	-	-	-		-	-	-
L	250	30	35	30	40	25	30	-	200
DL	500	300	315	300	360	225	270	-	-

** **B**: Battery, **G**: Diesel generator, **L**: Nondeferrable load, **DL**: Deferable load

The nondeferrable loads and the cold load are modeled as constant impedance loads. The deferrable loads in each building are modeled as dynamic PQ loads. As shown in Fig. 2, each building has more than one deferrable load, e.g., csCIu has 30, CCu3 has 17, CCu4 has 14, CCu5 has 28, CCu6 has 22, CCu7 has 22, and CCu8 has 5. In total, 138 deferrable loads will be dispatched and controlled by the NLM. Each deferable load reads the load profile (obtained from real-world measurements taken at the medical center), and the circuit breaker of the load is commanded by the NLM to open/close.

The most important part of the simulated EMT model is the modeling of the GFM inverters. All the battery inverters are modeled as a GFM inverter capable of forming the system voltage and frequency using droop control, and the PV inverters are modeled as GFL inverters to inject the desired amount of power. The control diagram of the GFM inverter is presented in Fig. 3. This is a very commonly used control algorithm for the GFM inverter, which has droop control to generate the V_d^*, frequency, ω^*, and phase angle, θ, double-loop control with voltage and current control loops, and the reverse Park transformation for the average inverter model. More details on the GFM control algorithm can be found in [10].

Modeling the GFM and GFL inverters individually is well studied; however, making the whole model work together and stabilizing it is a big challenge. In total, there are nine GFM inverters, two GFM diesel generators, and seven GFL PV inverters. The GFM inverters share the active and reactive power through droop control, and P_{ref} and Q_{ref} are the reference commands used to shift the frequency reference and voltage reference higher than nominal because the output power through power sharing will reduce the frequency and voltage. The strategy is to model the GFM inverters first and ensure that those models are stable and can achieve stable voltages and system frequency, and then to add the GFL inverter one by one.

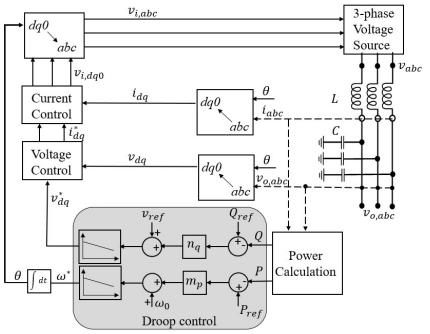

Fig. 3. Control diagram of the GFM battery inverter [10].

IV. Net Load Management Algorithm

The NLM engine is a central dispatch control (CDC) system that provides high-speed, cost-optimal coordination of a set of net loads (a combination of generation and deferrable loads) connected to the same electrical network [9]. Compared to existing load management solutions, the NLM control platform is superior in the optimal coordination process in applications with much larger numbers of net load resources and fast-changing generation resources. It is also capable of accurately meeting a specific aggregate power set point to generation resources while achieving dispatch on a faster timescale. The high-level objectives of the NLM-based CDC are to:

- Maintain system viability (generation capacity > load), including a specified generation reserve margin, by triggering dispatch actions each time the generation reserve margin falls below or above the target range.
- Minimize the overall cost (the sum of the unit cost change in the active power of the net load resource for all resources) of each dispatch action.
- Maximize the amount of deferrable load that is served using the available generation based on their priorities.

Table 2: Components in the cNLU for the NLM Engine

Component of cNLU	Number of Components
Deferrable load	138
Non-deferrable load	1 (8 loads are aggregated)
Solar GFL inverters	7
Slack bus	1 (8 GFM batteries + 2 diesel gen-set)
Grid	0 (off-grid mode)

NLM was previously demonstrated and validated to manage multiple net load units (NLUs), a combination of multiple GFL inverters, and deferrable and nondeferrable loads in grid-connected mode. In this work, however, the methodology is formulated so that NLM can be used for the optimal dispatch of NLUs operating on a microgrid in off-grid mode. The following formulation has been implemented to enable the NLM engine-based CDC for the concerned islanded microgrid network used in this paper. A combined NLU (cNLU) is defined here as an NLU that contains multiple nondeferrable loads combined into a single load with aggregated active power consumption; multiple deferrable loads with corresponding active power consumption; multiple solar GFL inverters with respective output active power; multiple droop-controlled GFM batteries combined into a single and aggregated active power resource called the *slack bus*; and active power consumption from the grid connection (zero in this off-grid mode). Table 2 lists the comprehensive set of net load elements of the microgrid under study. Each deferrable load and generating resource is associated with a preassigned participation unit cost. The generic optimization formulation used in this paper is as follows: Let the number of NLUs be N_u, with the i^{th} NLU having N_{d_i} deferable loads, a nondeferrable load, and N_{pv_i} PV inverters. The NLM engine optimization problem is given by:

$$\underset{x_{i,j},\,P_{pv_{i,j\Delta}}}{\text{minimize}} \sum_{i=1}^{N_u}\left[\sum_{j=1}^{N_{d_i}} c_{L_{i,j}} x_{i,j} P_{L_{i,j}} + \sum_{j=1}^{N_{pv_i}} c_{PV_{i,j}} \left|P_{pv_{i,j}}(t) - P_{pv_{i,j}}(t_0)\right|\right]$$

such that:

$$\sum_{i=1}^{N_u}\left[\sum_{j=1}^{N_{d_i}} (1-x_{i,j}) P_{L_{i,j}} + P_{c_i} - \sum_{j=1}^{N_{pv_i}} (P_{pv_{i,jbase}} + P_{pv_{i,j\Delta}})\right] = P^*_{slk}$$

$$P_{pv_{i,j\Delta,down}} \le P_{pv_{i,j\Delta}} \le P_{pv_{i,j\Delta,up}}, \forall i,j$$

$$P_{pv_{i,j\Delta}} = P_{pv_{i,j}}(t) - P_{pv_{i,j}}(t_0), \forall i,j$$

$$P^*_{slk} = P_{slk}(t) - P_{slk}(t_0)$$

$$x_{i,j} \in \{0,1\}, \forall i,j,$$

where $c_{L_{i,j}}$ and $c_{PV_{i,j}}$ are the participation unit costs for the j^{th} deferable load and the j^{th} PV inverter in the i^{th} NLU; t_0 is the time when the contingency happens; $P_{pv_{i,j\Delta,up}}$ and $P_{pv_{i,j\Delta,down}}$ are the upward and downward headroom of the j^{th} PV inverter in the i^{th} NLU; and $P_{L_{i,j}}$ and P_{c_i} are the load powers of the deferable loads and nondeferrable loads in the NLU i. $P_{pv_{i,j\Delta,up}}$ is determined by Algorithm 1 in [9], and $P_{pv_{i,j\Delta,down}} = -P_{pv_{i,jbase}}$, where, $P_{pv_{i,jbase}}$ is the initial operating power of the j^{th} PV inverter in NLU i before the contingency event. The optimization problem, with its mix of integer and real-valued decision variables, is simplified to a binary programming problem. The purpose of this relaxation is to solve the problem faster using dynamic programming rather than the standard mixed-integer linear programing.

The data flow and operation are shown in Fig. 4. The cNLU periodically sends its unit measurements (real-time power measurements of the deferable and nondeferable loads along with the generation measurements of the PV inverters, diesel genset, and GFM inverters with respective power capacities). The measurement data packet is sent via UDP channel to the central NLM engine every 0.1 s. The NLM engine algorithm, implemented using Python, uses this information to solve the abovementioned optimization problem in a fast timescale, determine an optimal net load allocation (a combination of on/off signals of deferrable loads and optimal power dispatch commands to the PV inverters) for the cNLU, and send it back via the UDP channel to the real-time simulator.

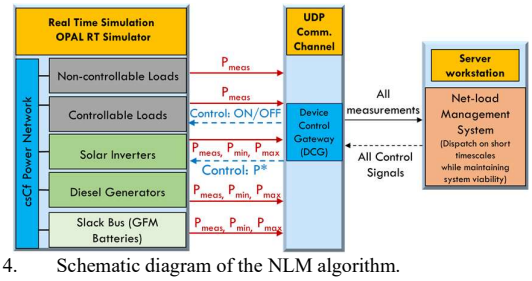

Fig. 4. Schematic diagram of the NLM algorithm.

V. Controller-Hardware-in-the-Loop

As shown in Fig. 1, there are two TI TMS320F28377D DSP boards. Each DSP board receives analog outputs (voltage and current) from the simulated PV inverter, runs the embedded current control algorithm, and sends the generated pulse-width modulation (PWM) digital signals to OPAL-RT to control the simulated inverter. The active power reference is also sent from OPAL-RT to the DSP through analog output.

This CHIL is established to evaluate the effectiveness of the current control algorithm in a real hardware microcontroller.

The PV inverter in CCu7 and MOB1 are selected for the CHIL evaluation. The average model is used instead of the switching model, and each inverter is connected to the grid through an L-filter. The three-phase output current and the point of common coupling voltage of each inverter are scaled and shifted to approximately 0–3 V, which are sent to the DSP through analog outputs together with the active power reference. The ePWM module in OPAL-RT converts the PWM digital inputs into the modulation index in the field-programmable gate array and sends those signals to the central processing unit to control the simulated inverter. The modulation index multiplies the DC voltage, thus generating the voltage references for the controlled voltage source for the average model.

VI. Implementaton and Results

A. Description of the Hardware-in-the-Loop Evaluation

The load profile for each building is obtained through the metering system by the energy management group of the University of Minnesota and is interpolated with a 30-second resolution based on the 1-second resolution raw data for a 15-minute test. Real-world solar irradiance data for the study are obtained for the area of the University of Minnesota from the National Renewable Energy Laboratory's (NREL's) solar Measurement and Instrumentation Data Center and NREL's National Solar Radiation Database, which aggregates data from a variety of solar measurement sites across the United States. The PV profile is also taken during the same time slot as the load profile, and it is interpolated into 10-second resolution to show the impact of fast-changing solar irradiance/PV generation on the NLM dispatch and coordination. The example loads and PV profile of csCIu are shown in Fig. 5.

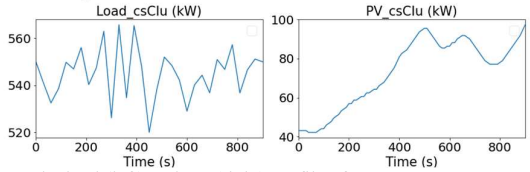

Fig. 5. The load (left) and PV (right) profile of csCIu.

This HIL setup includes three timescales: 1) the EMT simulation in OPAL-RT with a time step of 100 µs to demonstrate the transient dynamics and stability; 2) the NLM real-time dispatch with a time step of 5 seconds; and (3) the sampling and execution time step of 100 µs in TI DSP for the current control algorithm and the PWM generation.

The testing scenario is described as follows: 1) The community works in autonomous mode without the main grid support. 2) All the circuit breakers shown in Fig. 2 are closed, and all buildings are interconnected. 3) The battery inverters in each building operate in GFM mode and use droop control for power sharing. 4) Two contingency events occur during the test: The first contingency event happens at CCu6 when the 200-kVA battery inverter is disconnected at 5 minutes, and the second happens at CCu8 when the 50-kVA battery inverter is disconnected at 10 minutes. For all low-voltage buses at each building, the testing metrics are defined as: 1) voltage: (dynamic) outside the ITIC prohibited range (steady state), ±10% of nominal; 2) frequency: (dynamic) 58–61 Hz, (steady state) ±0.1 Hz.

B. Experimental Results

This section presents experiments that are designed to evaluate the performance of the NLM engine with the goal of serving at least 50% of the deferrable loads in csCIu and maintaining voltage and frequency within the target limits. The coordinated dispatch adjusts all net load statuses and operating levels across all buildings to rebalance the net load according to the priorities for starting the net load profile conditions. The representative results of the HIL testing are presented in Fig. 6–Fig. 10.

Fig. 6 shows the system frequency of the test. The results show that the system frequency is maintained within the target operating limits (59.9–60.1 Hz) during the whole test. In particular, the frequency is still maintained within the band (±0.1 Hz over nominal frequency, 60 Hz) during two contingency events. The 200-kVA battery inverter at CCu6 is disconnected at 300 seconds, and the frequency drops from 59.99 Hz to 59.95 Hz and slowly returns to the nominal values after the event with the contribution from other GFM inverters. The 50-kVA battery inverter at Ccu8 is disconnected at 600 seconds, and the frequency drops from 59.98 Hz to 59.97 Hz and returns to 59.98 Hz after the event.

The voltage of each building is presented in Fig. 7, which indicates that all the voltages are regulated within the target operation limits leveraged by the droop control and the NLM dispatch. For the two contingency events, all voltages drop slightly (≤6 V) the moment the contingency event occurs and return to a higher value and then stabilize. Note that the voltage of csCIu is the lowest of all the buildings because it serves the largest amount of load, and the voltage drop is the highest.

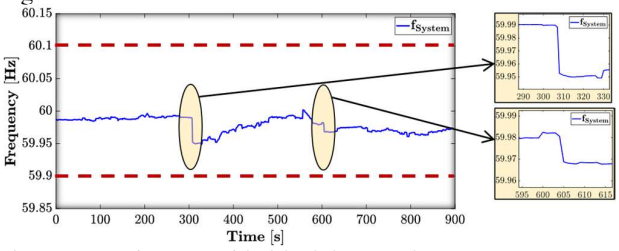

Fig. 6. System frequency of the islanded community.

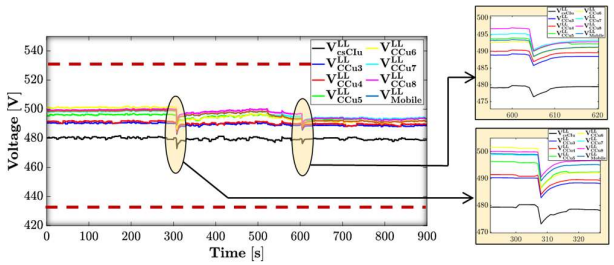

Fig. 7. Voltage at each building of the islanded community.

The active power measurements at the critical facility, csCIu, and other CCus are presented in Fig. 8 (a), (b), and (c) to demonstrate the performance of the NLM. The results illustrate the following: 1) csCIu meets a partial amount of the total active power demand by local emergency power resources, and csCIu imports the rest of the active power from the community's external network to meet the total demand; 2) CCus are cumulatively exporting the required amount of active power along with serving the cold load and all critical loads of their own; 3) the loss of power generation from two contingency events is quickly picked up and compensated by the rest of the GFM inverters through droop control and power sharing. Based on the calculation, approximately 70%–90% of the deferrable loads in csCIu are served, and 5%–10% of

the deferrable loads in the CCus are served. This means that we meet the target of serving at least 50% of the critical facility, csCIu. Overall, the NLM engine along with droop-controlled batteries ensure the viable and stable operation of the autonomous system and the continuous power supply of the critical facility by balancing generation and demand.

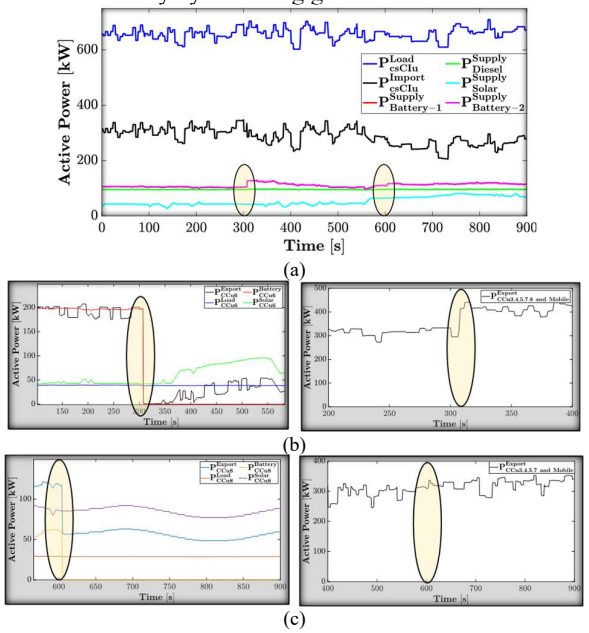

Fig. 8. Active power measurements at csCIu: (a) during the whole test; and (b) and (c) zoomed-in during the first and second contingency event.

Similarly, reactive power measurements at the critical facility, csCIu, and other CCus are presented in Fig. 9 (a), (b), and (c) to demonstrate the performance of the NLM for the reactive power balance. Similar observations to those of the active power measurements are obtained for the reactive power measurements. Thanks to the droop control for the reactive power sharing and NLM's balance of generation and load, the isolated community can achieve viable and stable operation to supply the power demand for the critical facility using local and neighbouring DERs.

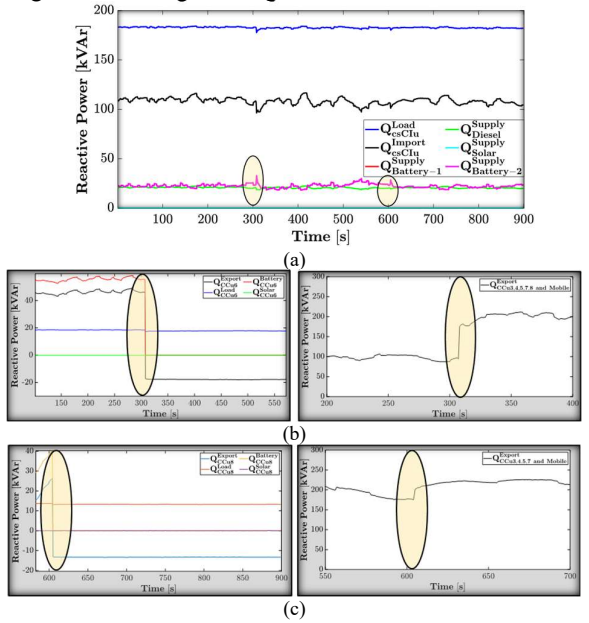

Fig. 9. Reactive power measurements at csCIu: (a) during the whole test; (b) and (c) zoomed-in during the first and second contingency event.

The active and reactive power response of one hardware controller evaluated through CHIL testing is presented in Fig. 10. The power references are noted as $Profile_{CCu7}^{Solar}$. The results show that the measured active and reactive power in OPAL-RT can track the power reference closely during the test, which indicates that the embedded current controller in TI DSP has satisfactory tracking performance.

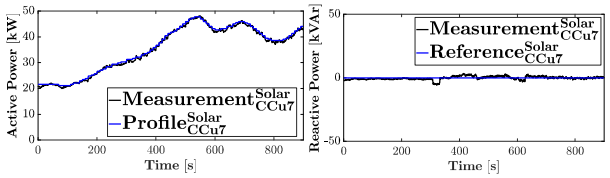

Fig. 10. The active and reactive power response of one hardware controller.

VII. Conclusions

This paper presents the performance evaluation of an NLM engine that balances load and generation in an isolated community to power the critical facility. A 15-minute test with two contingency events is performed to validate the NLM system. The results indicate that the measured system frequency and voltages meet the metrics, and the droop control for power sharing and the NLM's balance of generation and load can achieve viable and stable operation of the isolated community to supply the power demand for the critical facility. The NLM engine does not include secondary control of the GFM inverters for voltage and frequency stability, which is the limitation and will be included in our future work.

Acknowledgments

The authors thank Soumya Tiwari for her help with the CHIL setup.

References

[1] Jan Vrins, Global Energy Practice Lead, Distributed Energy Resource, https://www.navigant.com//media/www/site/downloads/energy/2016/distributedenergyresourcesimpactsonstrategybusines.pdf.

[2] J. Wang, et al., "Performance Evaluation of Distributed Energy Resource Management via Advanced Hardware-in-the-Loop Simulation," *IEEE Innovative Smart Grid Technologies Conference (ISGT),* 17-20 Feb. 2020, Washington DC, USA.

[3] S. Patel, M. Ahmed, and S. Kamalasadan, "A Novel Energy Storage-Based Net-Load Smoothing and Shifting Architecture for High Amount of Photovoltaic Integrated Power Distribution System," *IEEE Tran. Ind. Applications*, vol. 56, no. 3, May 2020, pp. 3090-3099.

[4] Jerzy Mikulik and Jacub Jurasz, "Net load variability with increased renewables penetration – simulation results for Poland," *2020 12th International Conference and Exibition on Electrical Power Quality and Utilisation (EPQU)*, 14-15 Sept. 2020, Cracow, Poland.

[5] M. Sun, et al., "Using Bayesian Deep Learning to Capture Uncertainty for Residential Net Load Forecasting," *IEEE Tran. Power Systems*, vol. 35, no.1, pp. 188-201, Jan. 2020.

[6] A. Alanazi, M. Alanazi, and A. Khodaei, "Managing the Microgrid Net Load Variability," *2016 IEEE/PES Transmission and Distribution Conference and Exposition (T&D)*, 3-5 May 2016, Dallas, USA.

[7] S. Kuppannagari, R. Kannan, and V. Prasanna, "NO-LESS: Near OptimaL CurtailmEnt Strategy Selection for Net Load Balancing in Micro Grids," *IEEE Innovative Smart Grid Technologies Conference (ISGT),* 19-22 Feb. 2020, Washington DC, USA.

[8] F. Elghitani, and E. EI-Saadany, "Smoothing Net Load Demand Variations Using Residential Demand Management," *IEEE Tran. Ind. Informatics,* vol. 15, no.1, pp. 390-398, Jan. 2019.

[9] B. Lundstrom, S. Patel and M. V. Salapaka, "Distribution Feeder-Scale Fast Frequency Response via Optimal Coordination of Net-Load Resources—Part I: Solution Design," *IEEE Transactions on Smart Grid*, vol. 12, no. 2, pp. 1289-1302, March 2021.

[10] J. Wang, N. Chang, X. Feng, and A. Monti, "Design of a Generalized Control Algorithm for Parallel Inverters for Smooth Microgrid Transition Operation," *IEEE Tran. Ind. Electron*., vol. 62, no. 8, Aug. 2015, pp. 4900-1914.